SCIENTIFIC REPORTS

OPEN

SUBJECT AREAS:
SODIUM CHANNELS
ION CHANNELS IN THE NERVOUS SYSTEM
NEUROPHYSIOLOGY
NATURAL PRODUCTS

Received
13 June 2013

Accepted
19 December 2013

Published
16 January 2014

Correspondence and requests for materials should be addressed to J.Y.H. (yhji@staff.shu.edu.cn)

PKA phosphorylation reshapes the pharmacological kinetics of BmK AS, a unique site-4 sodium channel-specific modulator

Z. R. Liu[1,2], H. Zhang[2], J. Q. Wu[2], J. J. Zhou[2] & Y. H. Ji[2,3]

[1]Department of Pharmacology, Institute of Medical Science, Shanghai Jiao Tong University School of Medicine, South Chongqing Road 280, Shanghai 200025, P.R.China, [2]Lab of Neuropharmacology and Neurotoxicology, Shanghai University, Nanchen Road 333, Shanghai 200436, P.R. China, [3]Shanghai Chongmin Xinhua Translational Institute of Cancer Pain, Nanmen Road 25, Shanghai 202151, P.R. China.

Although modulation of the activity of voltage-gated sodium channels (VGSCs) by protein kinase A (PKA) phosphorylation has been investigated in multiple preparations, the pharmacological sensitivity of VGSCs to scorpion toxins after PKA phosphorylation has rarely been approached. In this study, the effects of BmK AS, a sodium channel-specific modulator from Chinese scorpion *Buthus martensi* Karsch, on the voltage-dependent activation and inactivation of $Na_v1.2$ were examined before and after PKA activation. After PKA phosphorylation, the pattern of dose-dependent modulation of BmK AS, on both $Na_v1.2\alpha$ and $Na_v1.2$ ($\alpha + \beta1$) was reshaped. Meanwhile, the shifts in voltage-dependency of activation and inactivation induced by BmK AS were attenuated. The results suggested that PKA might play a role in different patterns how β-like toxins such as BmK AS modulate gating properties and peak currents of VGSCs.

cAMP-dependent protein kinase (PKA) has been long implicated to participate in central or peripheral nociceptive processing as secondary messenger[1]. The activity of VGSCs responsible for initiation and transmission of sensory signals was proved to be subjected to PKA-mediated phosphorylation[2]. However, the regulation patterns of VGSCs by PKA were divergent due to the various VGSCs subtypes and tissue- or cell-type distinct factors fine-tuning the physiological functions such as neuronal information encoding and transmission.

It has been well-documented that PKA phosphorylation could induce conformational change of VGSCs and influence the activity of VGSCs. PKA agonist inhibited the peak currents of VGSCs expressed in CHO cells by 40–50% and reduced the open probability of the channels[3]. Similarly, $Na_v1.2$, a brain-type VGSC subtype expressed in *Xenopus* oocyte was vulnerable to PKA phosphorylation as well. By perfusing cAMP agonist forskolin or isoproterenol (Iso), the intracellular cAMP level was increased leading to activation of PKA phosphorylation pathway in oocytes and inhibition of I_{Na} by ~20–30%[4]. In cardiac myocytes, activation of the β adrenergic system using Iso produced variable effects on I_{Na}, which were attributed to the activation of PKA[5].

BmK AS, originated from the venom of scorpion *Buthus martensii* Karsch (BmK), is a long chain toxin consisting of 66 amino acids cross-linked by four disulphide bridges[6], which shared highly similarity in sequence only with β anti-insect toxins AaH IT4 (from *Androctonus australis* Hector, AaH)[7] and BmK AS-1, thereby uniquely being classified as β-like toxins. The pharmacological binding assay revealed that the binding of BmK AS on mammalian or insect nerve preparations could be competently inhibited by BmK IT2, a site-4 VGSC-specific modulator, and therefore, the receptor site of these two toxins may functionally adjacent[8]. However, more evidences regarding to the molecular mechanism underlying the interaction of VGSCs with BmK AS remain to be clarified.

Earlier studies showed that BmK AS could substantially inhibit the Na^+ currents (I_{Na}) in neuroblastoma B104 cells[9]. Similarly, the reduction on I_{Na} was also observed in acutely dissociated small dorsal root ganglion (DRG) neurons from rats in the presence of BmK AS[10]. Later behavioral experiments on animal behavior demonstrated that BmK AS could relieve the nociceptive responses in inflammation pain models[11]. Recently, it is also found that hippocampal injection of BmK AS suppressed pentylenetetrazole-induced seizures in rat[12]. Thus, BmK AS seems

to suppress the cell excitability through direct modulation on VGSCs. Unexpectedly, several lines of evidences showed that BmK AS could promote the cell excitability. BmK AS was found to stimulate noradrenaline release from rat hippocampus slices by augmentation of sodium influx[13]. Electrophysiological studies also demonstrated that BmK AS could depolarized the voltage-dependence of fast or slow inactivation, resulting in slower inactivation[14].

Recent investigations revealed an interesting pharmacological characteristic of BmK AS which modulated the VGSCs in a unique U-shaped dose-dependent manner, i.e. at high concentrations, BmK AS increased the cell excitability, while at low concentrations, BmK AS suppressed the cell excitability[14]. The U-shaped relationship of VGSC modulation may be also dependent on VGSCs subtypes or tissue/cell environment.

In light of the potential role of some intracellular micro-environmental factors, such as PKA phosphorylation that was thought to be involving in regulating the channel activity, we examined whether PKA could play a role in BmK AS-driven modulation on $Na_v1.2$, the most abundant VGSC subtypes in brain tissues.

Results

PKA phosphorylation reshaped the modulation of BmK AS on I_{Na} amplitude. PKA phosphorylation was achieved by perfusion with β_2-adrenergic agonist isoproterenol (Iso) for 20 min following the procedures described by RD. Smith and AL.Goldin[15]. To understand if PKA phosphorylation may bring about any changes in $Na_v1.2$ current without co-expression with β_2-adrenergic receptor, experimental controls under different concentrations of Iso (10, 100 and 200 μM) were set up before the subsequent tests. The results proved that Iso at experimental range could affect neither the peak Na^+ currents (Supplementary Fig. S1, $p > 0.05$, $n = 4–7$) nor the voltage-dependent kinetics of $Na_v1.2$ (Supplementary Fig. S2). Therefore, 100 μM Iso was chosen to activate the PKA phosphorylation for $Na_v1.2$ with the co-expression of β_2-adrenergic receptor.

To observe the time course of the peak current change during PKA activation, I_{Na} was elicited by a depolarization step of −20 mV at an interval of 1 min lasting for 30 min in the presence of Iso. Baseline was established by perfusion with ND96 solution for 10 min before Iso administration (Fig. 1, open squares).

When applying with Iso, the peak currents of I_{Na} decreased gradually, reaching the equilibrium within 5 min (Fig. 1, Black bar, Pre Iso, open circles). After Iso treatment for 20 min, the Na^+ current amplitude was reduced by 12.04 ± 1.13% compared to the baseline (Fig. 1, Open circle). The Na^+ current did not further decrease, indicating that β_2-adrenergic receptors were saturated by Iso in oocytes.

However, application of 500 nM BmK AS resulted in a rapid decay in peak currents of I_{Na} in the initial 2.5 min and reached the equilibrium within 10 min (Fig. 1, Grey bar, Pre BmK AS, open triangles). The reduction rate of I_{peak} was 35.45 ± 4.57% by BmK AS at the time point of 20 min (Fig. 1, open triangles). The subsequent 100 μM isoproterenol perfusion produced additional 8.53 ± 1.28% reduction on I_{peak} (Fig. 1, Black bar, Pro Iso, open triangles). By contrast, if reversing the order of administration by pre-treatment with 100 μM Iso for 20 min, the following 500 nM BmK AS could only inhibit the I_{peak} by 18.02 ± 2.36% (Fig. 1,Grey bar, Pro BmK AS, open circles), far less evident when comparing to the pre-treatment of BmK AS. The reduction in I_{Na} appeared to be slow and unstable, indicating an attenuated efficacy of BmK AS on $Na_v1.2$ after PKA phosphorylation.

Previously, it has been well documented that BmK AS (0.1, 1, 10, 100, 500 nM) modulated the VGSCs in a unique U-shaped dose-dependent manner. To test if after PKA phosphorylation $Na_v1.2$ could be modulated by BmK AS in a similar way as seen in the case before, the effects of 1, 10 and 100 nM of BmK AS were examined on $Na_v1.2$ before and after PKA activation. Prior to Iso treatment, all the three concentrations of BmK AS could efficiently inhibit the peak currents of I_{Na} but to different extent (Fig. 2), with the most pronounced by 100 nM BmK AS which reduced the I_{peak} by 34.04 ± 4.27%, less evident by 1 nM (18.77 ± 2.65%) and the least by 10 nM (12.84 ± 2.33%), in accordance with the trend found in previous study (Fig. 2D). By contrast, this unique nonlinear dose-dependent reduction pattern of BmK AS was altered by pre-treatment with Iso. The reduction rate of BmK AS at three concentrations on I_{Na} were changed as follows: 1 nM BmK AS (20.81 ± 3.34%) ≈ 10 nM BmK AS (20.14 ± 3.89%) > 100 nM BmK AS (15.69 ± 2.65%), among which, the inhibitory potency of 100 nM BmK AS was largely attenuated after PKA activation and that of 10 nM BmK AS was slightly enhanced (Fig. 2D).

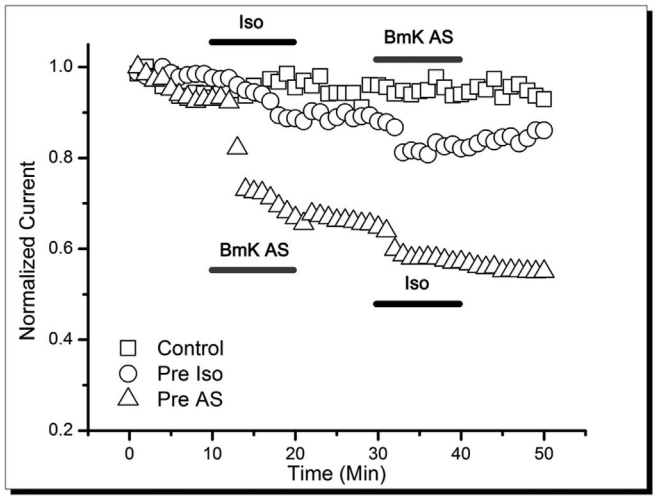

Figure 1 | Time course of peak sodium current amplitude during PKA activation. Peak sodium current amplitudes recorded from control (Open square), pre-administration of Iso (Open circle) and pre-administration of 500 nM BmK AS (Open triangle) are shown during 50-min time course.

PKA phosphorylation reshaped the nonlinear dose-dependent modulation of BmK AS on voltage dependence of activation. To qualify the pharmacological characters of BmK AS on $Na_v1.2$ before and after phosphorylation, samples were selected if the I_{Na} peaks at voltages between −20 and −10 mV in the I–V relationship. After perfusion with 100 nM BmK AS for 20 min, the I-V curve of I_{Na} was shifted to more negative position. A similar but not significant effect could also be observed in the presence of 1 nM BmK AS, while 10 nM BmK AS induced a slight opposite shift (Supplementary Fig. S3, left). However, when pre-treatment with Iso, the I-V curve of I_{Na} was shifted to the depolarized direction by 100 nM BmK AS, while that of 1 nM and 10 nM was shifted to the hyperpolarized positions (Supplementary Fig. S3, right).

Considering the fact that there may be an offset in I-V curve due to the variation in reversal potential (Vrev), the G-V relationship was further assessed to analyze the modulation of BmK AS on voltage-dependent activation of $Na_v1.2$ before and after PKA phosphorylation. Consistent with the nonlinear dose-dependent modulation of BmK AS found in I-V relationship, 100 nM BmK AS could competently shift the voltage-dependent activation to more negative potential ($\Delta V_{1/2} = 5.54$ mV, $P < 0.001$, Fig. 4A and Table 1) (Fig. 3C, left, Pre AS), while 10 nM BmK AS shifted the activation to the positive direction ($\Delta V_{1/2} = 4.89$ mV, $P < 0.001$, Fig. 4A and Table 1). Comparably, PKA activation almost abolished the hyperpolarized shift induced by 100 nM BmK AS on G-V curve after pre-treatment of Iso (Fig. 3C, left, Pro AS). But both 1 nM and 10 nM BmK AS could efficiently shift the voltage-dependent activation to more negative potentials whose $V_{1/2}$ was decreased by 3.31 mV ($P < 0.001$,

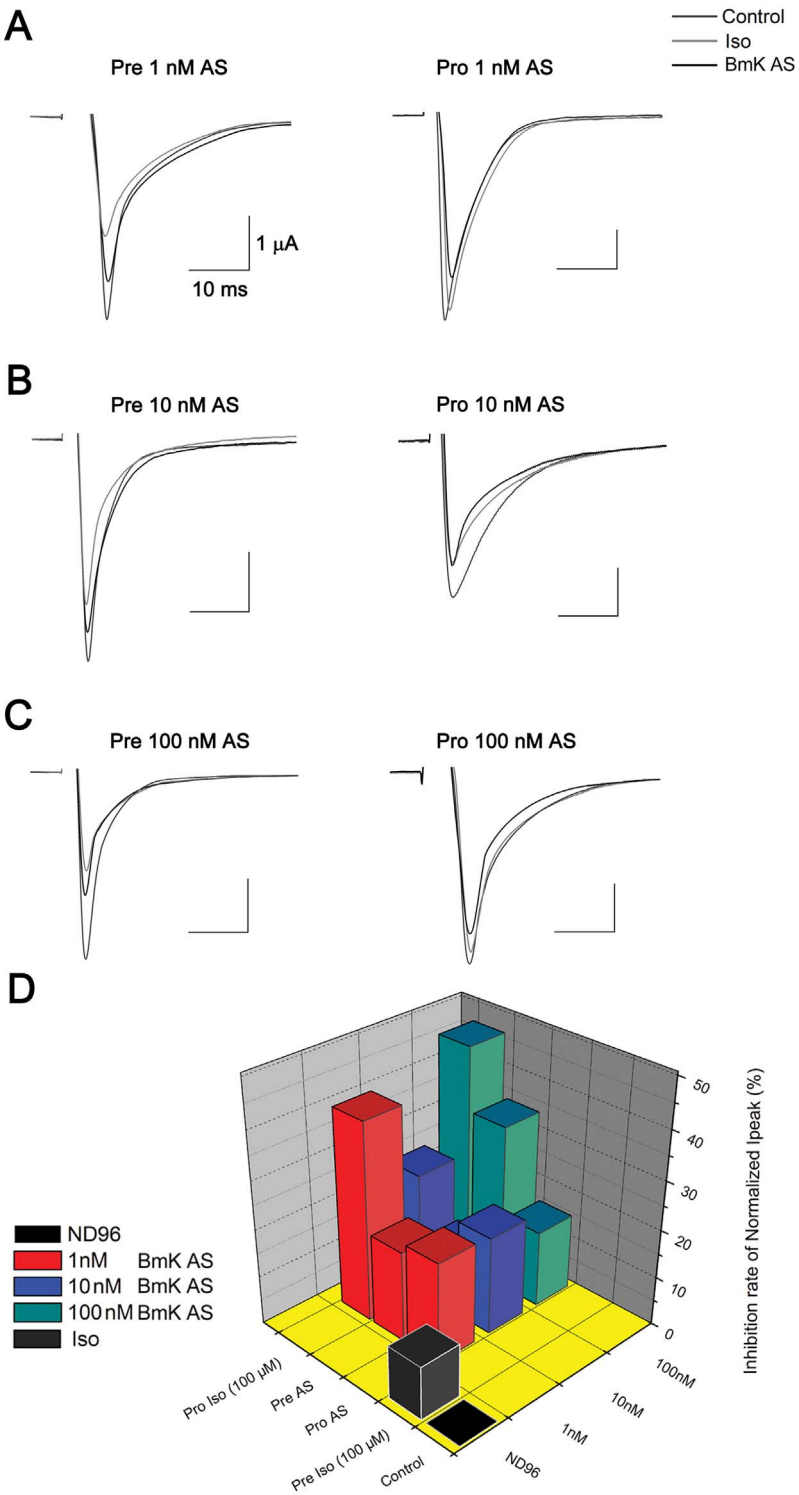

Figure 2 | BmK AS modulation of the sodium channel before and after PKA activation. (A–C), Representative sodium current traces after treatment of 1 nM,10 nM or 100 nM BmK AS (Black). (D). 3-D diagram illustrates the inhibition rate of BmK AS on $Na_v1.2\alpha$ before and after PKA activation.

Fig. 4A and Table 1) and 1.87 mV ($P > 0.05$, Fig. 4A and Table 1), respectively (Fig. 3A and B, left, Pro AS).

β1 subunit has been known to dramatically influence the gating properties of VGSCs, the modulation of BmK AS on voltage-dependent activation was studied in phosphorylated/unphosphorylated $Na_v1.2$ ($\alpha + \beta1$) in parallel to the $Na_v1.2\alpha$ expressed alone. Distinctively different with the case observed in $Na_v1.2\alpha$, BmK AS could move the voltage dependent activation of $Na_v1.2$ ($\alpha + \beta1$) towards depolarization in a linear dose-dependent way (Fig. 3A–C, right, Pre AS): Prominent for 100 nM ($\Delta V_{1/2} = 6.43$ mV, $P < 0.001$) and 10 nM ($\Delta V_{1/2} = 6.03$ mV, $P < 0.005$), but less significant for 1 nM ($\Delta V_{1/2} = 2.05$ mV, $P < 0.05$) (Fig. 4A and Table 1). Similar with $Na_v1.2\alpha$, after PKA activation, the modulation of BmK AS on voltage dependent of activation became far less evident (Fig. 3A–C, right, Pro AS), only 10 nM BmK AS caused depolarized shift on $V_{1/2}$ ($\Delta V_{1/2} = 4.34$ mV, $P < 0.05$) (Fig. 4A and Table 1). Thus, PKA

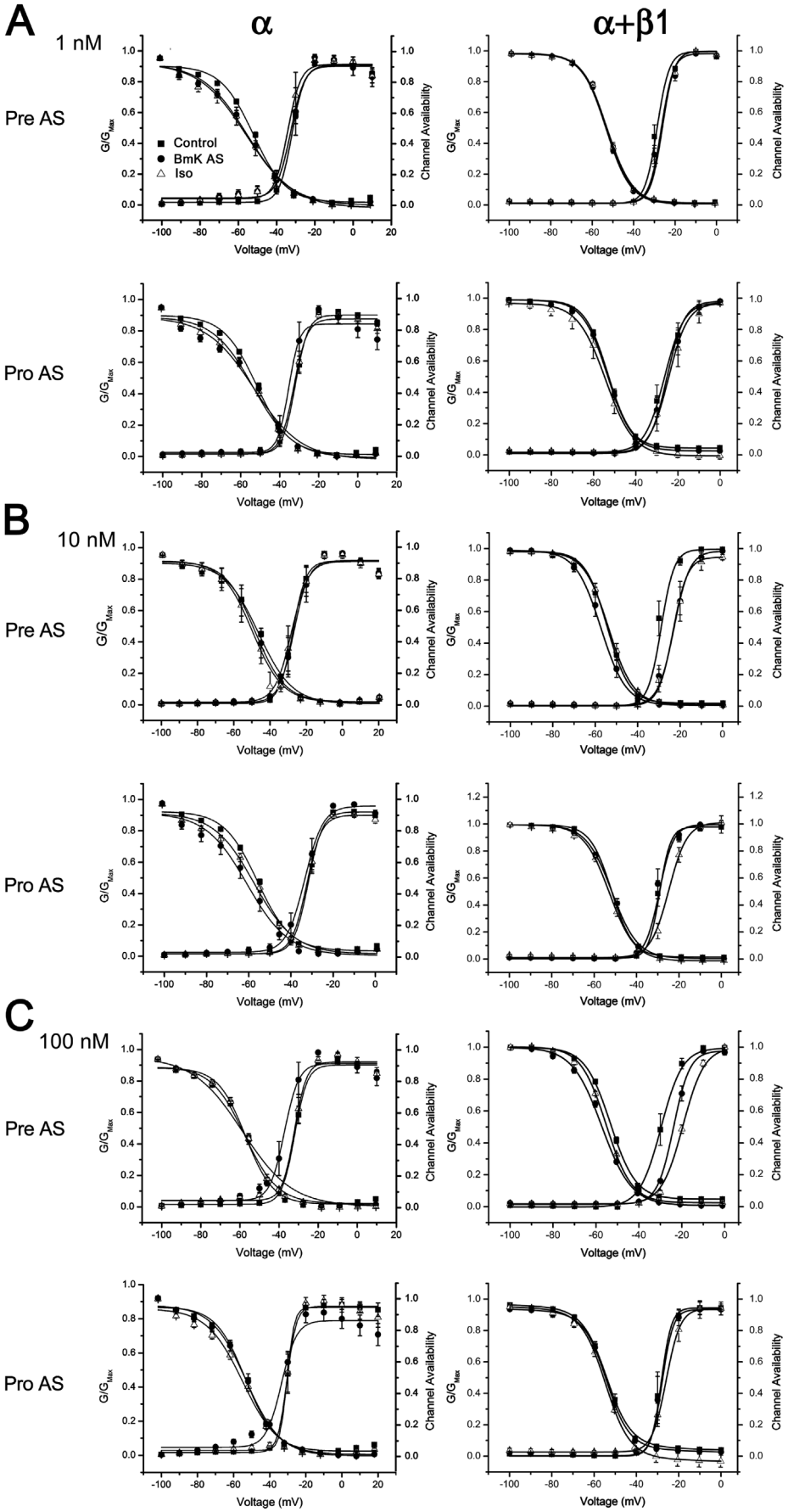

Figure 3 | Voltage dependence of activation and inactivation for $Na_v1.2$ sodium channels. The voltage-dependence of activation and inactivation are shown for α subunits alone (Left pannel) and (α + β1) subunits (Right pannel).

Table 1 | Parameters for voltage-dependence of activation and inactivation of $Na_v1.2\alpha$ expressed in *Xenopus laevis* oocytes.

BmK AS Concentration[1]	Administration[2]	Activation			Steady-state inactivation		
		$V_{1/2}$ (mV)	k_m (mV)	N[3]	$V_{1/2}$ (mV)	k_m (mV)	N
1 nM	Control	−32.15 ± 0.48	3.12 ± 0.45	49	−51.23 ± 0.79	8.49 ± 0.71	25
	Pre AS	−32.57 ± 0.85	3.61 ± 0.72	5	−54.46 ± 1.03*	11.65 ± 0.97*	7
	Pro Iso	−34.19 ± 0.75*	3.39 ± 0.49	5	−54.73 ± 1.30	12.39 ± 1.24*	6
	Pre Iso	−33.03 ± 0.67	3.25 ± 0.51	29	−53.03 ± 1.06	9.93 ± 0.96	36
	Pro AS	−35.46 ± 0.94***	2.78 ± 0.51	7	−52.58 ± 1.61	12.04 ± 1.54*	8
10 nM	Pre AS	−27.26 ± 0.86***	3.78 ± ± 0.71	8	−53.16 ± 0.85	7.38 ± 0.74	7
	Pro Iso	−28.10 ± 0.78**	4.56 ± 0.71*	8	−54.44 ± 0.86*	7.48 ± 0.86	8
	Pre Iso	−33.03 ± 0.67	3.25 ± 0.51	29	−53.03 ± 1.06	9.93 ± 0.96	36
	Pro AS	−34.02 ± 0.91	4.01 ± 0.68	11	−56.53 ± 1.49**	10.61 ± 1.37*	10
100 nM	Pre AS	−37.69 ± 1.09***	3.26 ± 0.99	8	−51.72 ± 0.59	8.24 ± 0.52	10
	Pro Iso	−32.16 ± 0.57	3.09 ± 0.54	7	−51.07 ± 0.57	8.87 ± 0.51	10
	Pre Iso	−33.03 ± 0.67	3.25 ± 0.51	29	−53.03 ± 1.06	9.93 ± 0.96	36
	Pro AS	−33.53 ± 1.01	4.21 ± 0.80*	7	−51.10 ± 0.71	9.48 ± 0.64	9
		Fast inactivation			Slow inactivation		
		$V_{1/2}$ (mV)	k_m (mV)	N	$V_{1/2}$ (mV)	k_m (mV)	N
1 nM	Control	−31.51 ± 0.97	10.49 ± 0.87	23	−47.16 ± 1.06	9.70 ± 0.93	22
	Pre AS	−35.04 ± 0.66*	13.37 ± 0.38*	10	−50.20 ± 0.56*	13.59 ± 0.48*	12
	Pro Iso	−37.32 ± 2.50*	17.11 ± 2.70*	6	−49.29 ± 0.97	12.35 ± 0.91	7
	Pre Iso	−30.93 ± 1.18	11.26 ± 1.07	27	−47.45 ± 1.32	10.49 ± 1.17	32
	Pro AS	−35.98 ± 0.88*	8.24 ± 0.77	6	−47.39 ± 2.68	14.67 ± 2.81*	7
10 nM	Pre AS	−32.30 ± 0.85	8.90 ± 0.75	8	−51.37 ± 0.92*	8.35 ± 0.80	8
	Pro Iso	−34.43 ± 0.90	9.00 ± 0.79	8	−52.26 ± 0.90**	9.08 ± 0.80	8
	Pre Iso	−30.93 ± 1.18	11.26 ± 1.07	27	−47.45 ± 1.32	10.49 ± 1.17	32
	Pro AS	−28.09 ± 3.67	18.88 ± 3.67**	12	−50.28 ± 0.65*	9.40 ± 2.67	11
100 nM	Pre AS	−36.89 ± 1.19**	12.91 ± 1.15	9	−46.81 ± 1.24	11.42 ± 1.16	9
	Pro Iso	−32.17 ± 1.06	12.09 ± 0.97	10	−47.52 ± 0.86	11.09 ± 0.79	10
	Pre Iso	−30.93 ± 1.18	11.26 ± 1.07	27	−47.45 ± 1.32	10.49 ± 1.17	32
	Pro AS	−29.42 ± 0.80	10.75 ± 0.72	8	−47.38 ± 0.56	10.03 ± 0.50	9

[1]Kinetic parameters of $Na_v1.2\alpha$ after applying with BmK AS of different concentrations (1, 10 and 100 nM) were listed as Mean ± SEM separately.
[2]All the concentrations of BmK AS were applied before (Pre AS) and after (Pro AS) PKA activation through perfusion with 100 μM Iso.
[3]N indicates the number of samples tested.
*, ** and *** indicates significant difference between control and BmK AS or Iso treated oocytes (*, $P < 0.05$; **, $P < 0.01$; ***, $P < 0.001$; t-test).

phosphorylation largely attenuated the effect of BmK AS on voltage-dependent activation of $Na_v1.2$ either co-expressed with β1 subunit or not.

PKA phosphorylation reshaped the nonlinear dose-dependent modulation of BmK AS on voltage dependence of inactivation. Accordingly, the modulation of BmK AS on steady-state inactivation of $Na_v1.2\alpha$ was assessed before and after PKA phosphorylation. Generally, the steady-state inactivation of $Na_v1.2\alpha$ was less sensitive to the modulation of BmK AS compared to that of activation (Fig. 3, left). Among the three dosages of BmK AS applied, only 1 nM BmK AS moderately shifted the value of $V_{1/2}$ to more negative direction ($\Delta V_{1/2} = 3.23$ mV, $P < 0.05$). But following with PKA phosphorylation, the results showed that the modulation of 10 nM BmK AS was substantially enhanced, which hyperpolarized the voltage-dependent steady-state inactivation by 5.30 mV ($P < 0.01$) (Table 1, Fig. 3B and 4A). It was of notice that BmK AS at higher concentration (100 nM) did not shift the steady-state inactivation curve before and after PKA phosphorylation.

In contrast to the case of $Na_v1.2\alpha$, BmK AS had a greater impact on the steady-state inactivation of $Na_v1.2$ (α + β1) in a dose dependent manner. As shown in table 1 and figure 4A, both 10 nM and 100 nM BmK AS could efficiently hyperpolarize the steady-state inactivation ($\Delta V_{1/2} = 3.03$ mV for 10 nM, $P < 0.001$; $\Delta V_{1/2} = 4.04$ mV for 100 nM, $P < 0.001$). However, these two concentrations of BmK AS barely had any influence on steady-state inactivation of $Na_v1.2$ (α + β1) after PKA activation, whereas 1 nM BmK AS imposed a slight but significant leftward shift on $V_{1/2}$ ($P < 0.05$, Table 1).

For the sodium channels expressed in *Xenopus* oocytes, the voltage dependent of inactivation splits into two inactivated components, with the faster one whose decaying currents last for several milliseconds and slower one lasts for dozens of milliseconds (see below). It was therefore analyzing the modulation of BmK AS on voltage dependent fast and slow inactivation separately before and after PKA phosphorylation. In oocytes expressed with $Na_v1.2\alpha$, it was surprised to found that BmK AS hyperpolarized the $V_{1/2}$ values of fast and slow inactivation in an opposite way. At high (100 nM) and low concentrations (1 nM), BmK AS could induce a remarkable hyperpolarized shift in $V_{1/2}$ for fast inactivation but not slow inactivation, whereas this shift in slow inactivation was more evident than in fast inactivation by BmK AS at intermediate concentration (10 nM) (Fig. 4B, left, Pre AS; Fig. S4; Table 1). However, the effects of BmK AS on both inactivated state were greatly attenuated after PKA activation (Fig. 4B, left, Pro AS; Fig. S4; Table 1).

Contrary to the difference in BmK AS modulations in voltage-dependent activation between $Na_v1.2\alpha$ and $Na_v1.2$ (α + β1), both fast and slow inactivation of $Na_v1.2$ (α + β1) was subjected to BmK AS modulation in a linear dose-dependent way. Notably, the extent of hyperpolarized shift in $V_{1/2}$ induced by 100 nM BmK AS did not increase much compared with the shift induced by 10 nM BmK AS, but both of which were substantially larger than that of 1 nM BmK AS (Fig. 4B, right, Pre AS; Fig. S5; Table 2). Meanwhile, the slow inactivation was more affected by BmK AS at efficient dose range (10 nM and 100 nM) than the fast inactivation. As expected due to the findings mentioned above, the prominent effects of BmK AS for

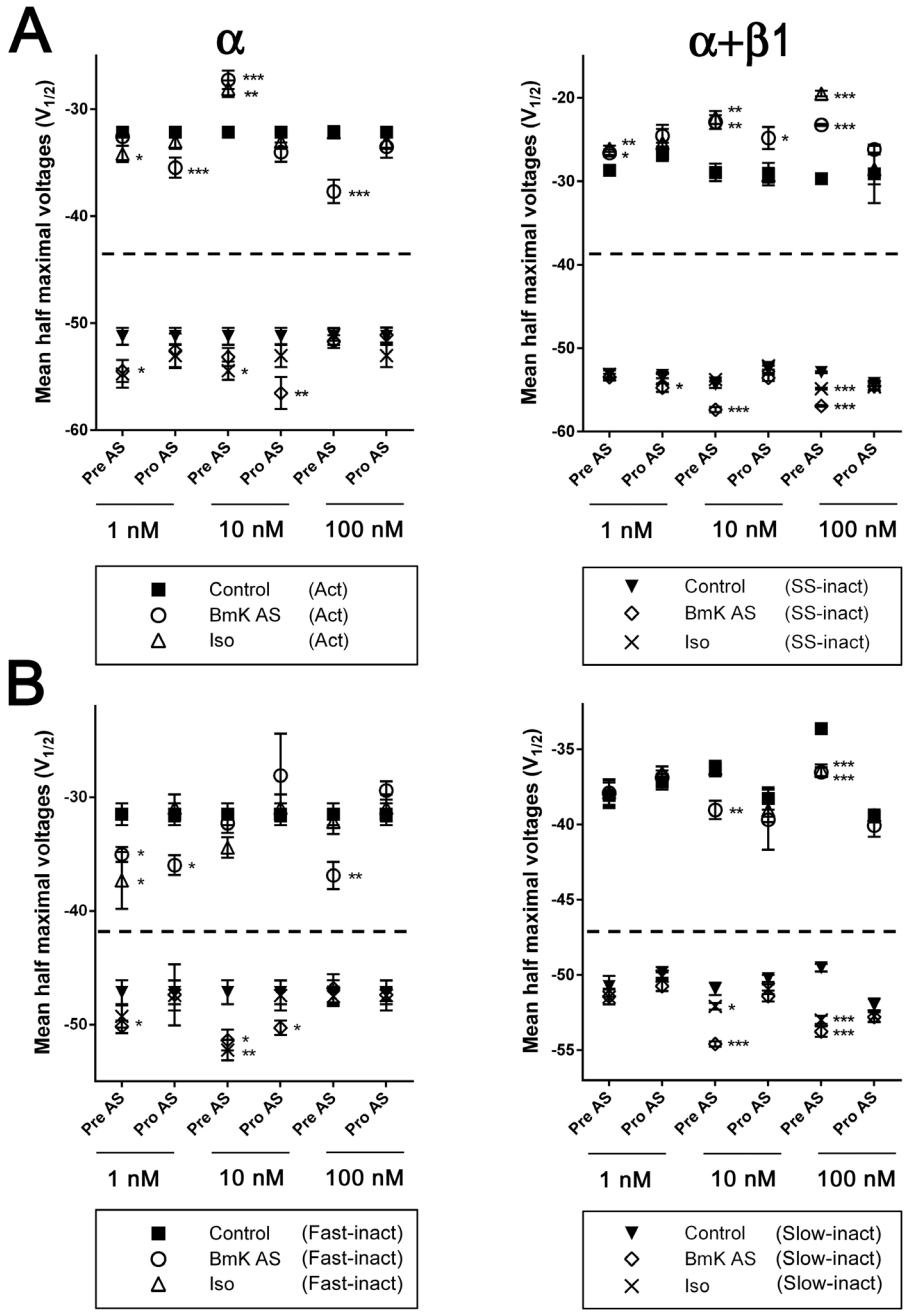

Figure 4 | Kinetics for voltaged dependent activation and inactivation for $Na_v1.2$ sodium channels.

both fast and slow inactivation were inevitably removed after PKA activation (Fig. 4B, right, Pro AS; Fig. S5; Table 2).

PKA phosphorylation reshaped the modulation of BmK AS on open state inactivation kinetics inactivation. As mentioned above, the fast and slow inactivated components of Na^+ currents of $Na_v1.2$ responded differentially to BmK AS. To evaluate the fast and slow inactivation kinetics in the presence of BmK AS before and after PKA phosphorylation, we analyzed the time constants and fraction of fast component for inactivation.

For $Na_v1.2\alpha$, at most of the potentials tested, both 1 nM and 100 nM BmK AS could accelerate the open-state fast inactivation by reducing the time constant (τ_{fast}) −20 to +20 mV; $P < 0.1$). In terms of 10 nM BmK AS, it could effectively delay the inactivation by increasing the time constants of slow inactivation (τ_{slow}) and transform a proportion of Na^+ currents from the fast-inactivation component into the slow-inactivation component at higher depolarized potentials (+10 to +20 mV, $P < 0.05$) (Fig. 5A, left, Pre AS). Hence, the inactivation kinetics of $Na_v1.2\alpha$ was modulated by BmK AS in a bidirectional manner. However, when PKA was pre-activated, it was found that the sensitivity of fast inactivation to BmK AS was distinctly attenuated. BmK AS at 1 nM and 100 nM BmK AS could even increase the time constant of slow inactivation at 0 mV and 10 mV respectively (Fig. 5A and 5C, left, Pro AS).

Likewise, the linear dose-dependent modulation of BmK AS on inactivation kinetics of $Na_v1.2$ ($\alpha + \beta1$) was reshaped after PKA activation, in agreement with the cases found in voltage-dependent activation and inactivation. Unlike the effect on $Na_v1.2\alpha$, 10 nM BmK AS induced a slight decrease in τ_{fast} (−10 mV, $P < 0.1$) but distinctive increase the τ_{slow} (−30 mV, $P < 0.05$) for $Na_v1.2$ ($\alpha + \beta1$) at more negative potentials after PKA activation. In the presence of 100 nM BmK AS, the fraction of fast component of inactivation at −30 mV and −20 mV were greatly suppressed, while a substantial increase in τ_{fast} could also be seen at −30 mV (Fig. 5B and 5C, right,

Table 2 | Parameters for voltage-dependence of activation and inactivation of $Na_v1.2$ ($\alpha + \beta1$) expressed in *Xenopus laevis* oocytes

BmK AS Concentration[1]	Administration[2]	Activation			Steady-state inactivation		
		$V_{1/2}$ (mV)	k_m (mV)	N[3]	$V_{1/2}$ (mV)	k_m (mV)	N
1 nM	Control (Pre AS)	−28.66 ± 0.52	2.91 ± 0.34	5	−53.10 ± 0.42	5.82 ± 0.21	6
	Pre AS	−26.61 ± 0.42*	2.89 ± 0.65	6	−53.46 ± 0.41	5.80 ± 0.24	6
	Pro Iso	−26.11 ± 0.37**	2.84 ± 0.32	6	−53.12 ± 0.55	6.14 ± 0.28	6
	Control (Pro AS)	−26.65 ± 0.79	4.645 ± 0.29	6	−53.25 ± 0.35	5.51 ± 0.18	6
	Pre Iso	−25.40 ± 2.16	4.14 ± 0.67	6	−53.66 ± 0.57	5.85 ± 0.32	6
	Pro AS	−24.56 ± 0.82	4.53 ± 0.25	5	−54.72 ± 0.51*	6.61 ± 0.34*	6
10 nM	Control (Pre AS)	−28.94 ± 1.05	3.07 ± 0.55	5	−54.33 ± 0.43	5.22 ± 0.51	7
	Pre AS	−22.91 ± 0.82**	3.70 ± 0.90	6	−57.36 ± 0.31***	5.90 ± 0.15	5
	Pro Iso	−22.38 ± 0.78**	3.41 ± 2.00	4	−53.75 ± 0.24	5.79 ± 0.12	4
	Control (Pro AS)	−29.15 ± 1.35	2.61 ± 0.49	8	−52.53 ± 0.43	5.14 ± 0.23	8
	Pre Iso	−29.29 ± 0.87	3.34 ± 0.32	7	−52.10 ± 0.46	6.05 ± 0.28	6
	Pro AS	−24.81 ± 1.31*	4.28 ± 0.45*	8	−53.55 ± 0.36	6.13 ± 0.34*	8
100 nM	Control (Pre AS)	−29.68 ± 0.58	4.45 ± 0.61	6	−52.87 ± 0.11	6.12 ± 0.13	6
	Pre AS	−23.25 ± 0.12***	3.78 ± 0.10	6	−56.91 ± 0.09***	7.01 ± 0.06***	6
	Pro Iso	−19.49 ± 0.32***	5.03 ± 0.28	6	−54.84 ± 0.12***	6.04 ± 0.10	6
	Control (Pro AS)	−29.11 ± 3.50	2.40 ± 1.21	5	−54.20 ± 0.36	6.23 ± 2.09	7
	Pre Iso	−28.57 ± 1.80	2.60 ± 0.59	4	−54.62 ± 0.45	5.79 ± 0.29	7
	Pro AS	−26.17 ± 0.41	3.35 ± 0.14	4	−54.55 ± 0.42	6.24 ± 0.36	5
		Fast inactivation			Slow inactivation		
		$V_{1/2}$ (mV)	k_m (mV)	N	$V_{1/2}$ (mV)	k_m (mV)	N
1 nM	Control (Pre AS)	−38.05 ± 0.85	8.80 ± 0.53	6	−50.76 ± 0.69	7.38 ± 0.38	6
	Pre AS	−37.90 ± 0.90	8.75 ± 0.56	6	−51.43 ± 0.52	6.68 ± 0.26	6
	Pro Iso	−37.87 ± 0.82	8.67 ± 0.54	6	−51.46 ± 0.49	6.85 ± 0.28	6
	Control (Pro AS)	−37.16 ± 0.52	8.75 ± 0.34	6	−49.83 ± 0.36	6.13 ± 0.31	5
	Pre Iso	−36.57 ± 0.43	8.52 ± 0.34	6	−50.08 ± 0.26	7.05 ± 0.30	5
	Pro AS	−36.88 ± 0.48	8.11 ± 0.33	5	−50.74 ± 0.32	6.83 ± 0.19	5
10 nM	Control (Pre AS)	−36.25 ± 0.32	7.02 ± 0.39	7	−50.92 ± 0.41	6.70 ± 0.26	5
	Pre AS	−39.03 ± 0.61**	9.01 ± 0.41**	7	−54.58 ± 0.18***	6.72 ± 0.18	7
	Pro Iso	−36.28 ± 0.51	7.95 ± 0.38	5	−52.08 ± 0.22*	6.71 ± 0.11	5
	Control (Pro AS)	−38.27 ± 0.74	8.23 ± 0.58	8	−50.23 ± 0.24	7.15 ± 0.26	8
	Pre Iso	−39.05 ± 0.79	9.03 ± 0.60	7	−50.94 ± 0.32	6.69 ± 0.26	8
	Pro AS	−39.68 ± 2.00	8.86 ± 0.85	8	−51.40 ± 0.36	7.01 ± 0.29	8
100 nM	Control (Pre AS)	−33.62 ± 0.23	8.14 ± 0.25	6	−49.51 ± 0.26	7.51 ± 0.31	6
	Pre AS	−36.52 ± 0.33***	10.11 ± 0.38**	6	−53.76 ± 0.35***	7.82 ± 0.38	6
	Pro Iso	−36.39 ± 0.38***	9.65 ± 0.46*	6	−52.98 ± 0.27***	7.87 ± 0.22	6
	Control (Pro AS)	−39.49 ± 0.31	9.12 ± 0.37	6	−52.00 ± 0.43	7.17 ± 0. 45	6
	Pre Iso	−39.37 ± 0.38	8.83 ± 0.47	7	−52.74 ± 0.39	6.64 ± 0.27	6
	Pro AS	−40.07 ± 0.74	9.65 ± 0.52	5	−52.80 ± 0.34	7.28 ± 0.32	5

[1]Kinetic parameters of $Na_v1.2$ ($\alpha + \beta1$) after applying with BmK AS of different concentrations (1, 10 and 100 nM) were listed as Mean ± SEM separately.
[2]All the concentrations of BmK AS were applied before (Pre AS) and after (Pro AS) PKA activation through perfusion with 100 μM Iso.
[3]N indicates the number of samples tested.
*, ** and *** indicates significant difference between control and BmK AS or Iso treated oocytes (*, $P < 0.05$; **, $P < 0.01$; ***, $P < 0.001$; t-test).

Pre AS). However, these changes almost disappeared after PKA activation (Fig. 5B and 5C, right, Pro AS). In addition, it was relevant to note that BmK AS did not change the amount of slowly inactivating steady-state Na^+ currents featured for $Na_v1.2$ after depolarization to −20 mV for 10 ms. Unexpectedly, a slight but visible increase in steady-state Na^+ currents could be induced by 10 nM or 100 nM BmK AS after 10 ms depolarization ($P < 0.05$) (Fig. 6).

Discussion

The current study demonstrated that PKA activation could reshape the dose-dependent modulation of BmK AS, a β-like scorpion toxin, on $Na_v1.2$ expressed in oocytes. The finding suggested that the potency of toxins on sodium channel was different before and after PKA phosphorylation.

Based on the previous pharmacological studies of BmK AS on sodium channels, it was concluded that the voltage-dependent activation and inactivation of these VGSC subtypes displayed a U-shaped shift in response to different concentration of BmK AS (0.1, 1, 10, 50, 100, 500 nM)[14,16]. In the current research, three of the concentrations of BmK AS (1, 10 and 100 nM) were chosen to investigate the pharmacological characteristics of BmK AS on $Na_v1.2\alpha$ with or without β1 subunit. It was found that co-expression of β1 subunit abolished the U-shape dose-dependence of BmK AS. The modulation of BmK AS on $Na_v1.2$ was attenuated after PKA activation regardless of co-expression with β1 subunit or not. The results suggested that complex interactions might exist among three factors: extracellular scorpion toxin, intracellular PKA, and crossing-membrane β1 subunit.

The results showed that both 1 nM and 100 nM BmK AS could facilitate the activation of $Na_v1.2\alpha$ through negatively shifting the voltage-dependent activation, while 10 nM BmK AS induced a shift in activation to the opposite direction. This nonlinear modulation of BmK AS could also be observed on voltage-dependent fast and slow inactivation of $Na_v1.2\alpha$, in which the inactivation curves were both negatively shifted by 1 nM or 100 nM BmK AS but not by 10 nM BmK AS. Although only three concentrations of BmK AS tested, this nonlinear modulation character of BmK AS was consistent with the U-shaped dose-dependent effects of BmK AS in previous researches.

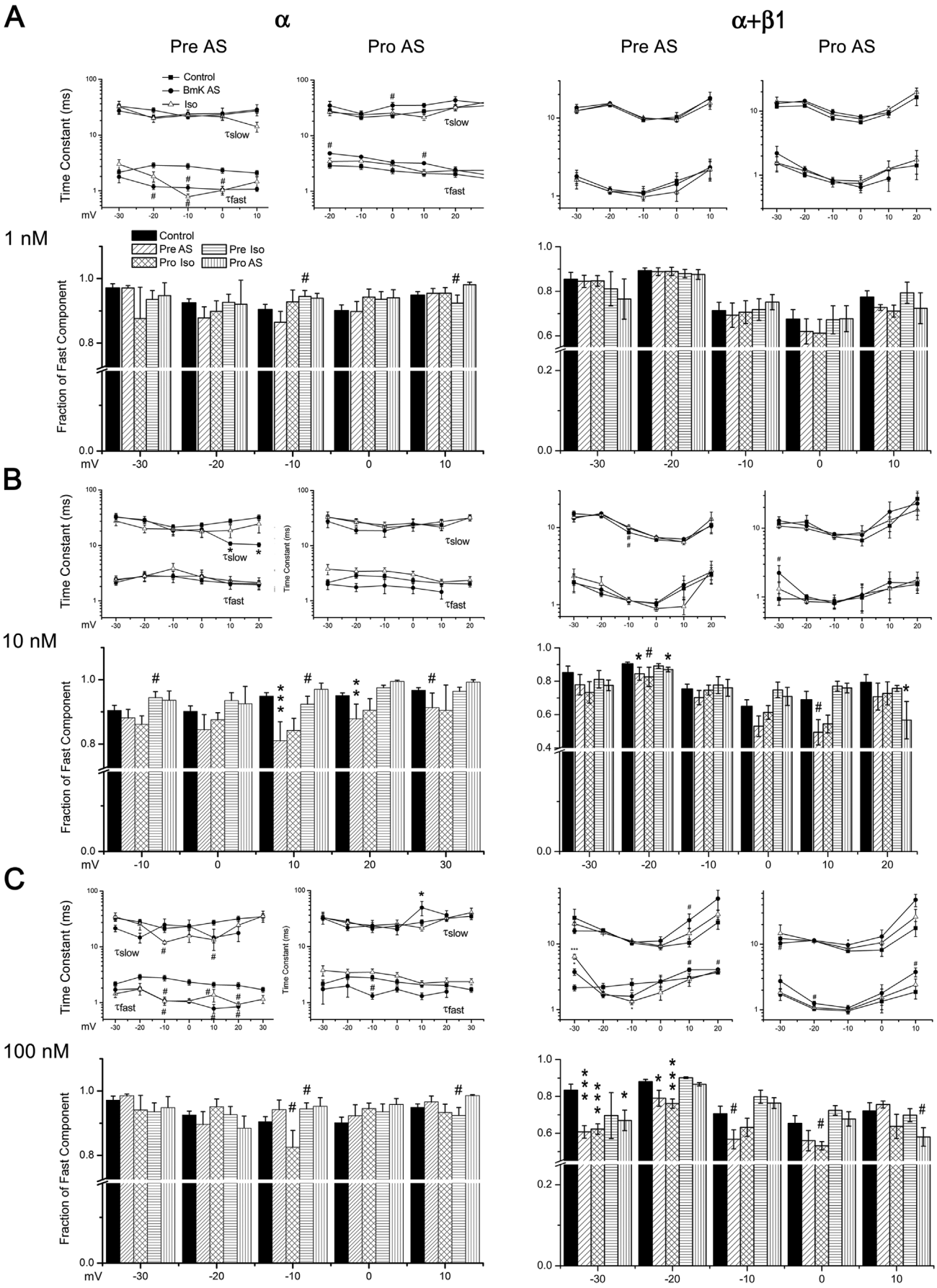

Figure 5 | Modulation of BmK AS on the inactivation kinetics of phosphorylated/non-phophorylated $Na_v1.2$. (A–C) Inactivation time constants and fraction of fast component modulated by BmK AS of each concentration (1, 10 and 100 nM).

However, the direction of shift induced by BmK AS on voltage-dependent activation/inactivation is opposite in two different VGSCs expression systems, a depolarized direction in *Xenopus* oocytes but a hyperpolarized direction in ND7-23 cells (in both expression system, the concentrations of BmK AS applied were the same). Although the opposite direction of shift could be attributed to the different VGSC subtypes, the possibilities of intracellular micro-environment should also be taken into consideration. For example, background PKA activity may be different between systems and therefore cause different effects[17].

In contrast with activation, the hyperpolarized shift of voltage-dependent inactivation of $Na_v1.2\alpha$ by BmK AS could be reproduced on $Na_v1.2$ ($\alpha + \beta1$). Nevertheless, the dose-dependent character of BmK AS modulation on $Na_v1.2$ ($\alpha + \beta1$) was quite different with that of $Na_v1.2\alpha$. The results showed that the efficacy of BmK AS on voltage-dependent activation/inactivation increased in a linear way with the rise of concentrations applied with (1–100 nM). Meanwhile, in oocytes expressed with $Na_v1.2$ ($\alpha + \beta1$), the shift in activation induced by BmK AS were different from that in oocytes expressed with $Na_v1.2\alpha$ only. This difference could be explained by the co-expression of β1 subunit which has been reported to positively move the voltage-dependence of activation and accelerate the inactivation for $Na_v1.2$[18].The disappeared nonlinear modulation of BmK AS and the decreased inactivation time on $Na_v1.2$ ($\alpha + \beta1$) in this study may be caused by the removal of the component of an intermediate inactivation mode brought by *Xenopus* oocytes injection which was substantially reduced through co-injection of β1 subunit[19–21].

One interesting finding was that BmK AS at different concentrations may result in different shifts in inactivation kinetics on both $Na_v1.2\alpha$ and $Na_v1.2$ ($\alpha + \beta1$) determined with 10 ~ 600 ms-long conditioning pulses (See results). One possibility is that the binding affinity of BmK AS may vary with the duration of depolarized stimuli which was common among scorpion α toxins but rarely on β toxins[22]. However, direct evidences correlating the relationship between binding affinity of BmK AS and different sodium channel states remain to be studied in the future.

The effects of sodium channels on electrical excitability of a neuron depend on both the kinetics and voltage dependence of sodium channel activation and inactivation[18]. In accordance with the previous reports, the voltage-dependent activation and inactivation of $Na_v1.2\alpha$ were not affected by the PKA regulation[23], which held to be true for the case of $Na_v1.2\alpha$ co-expression with the β1 subunit as well. However, PKA phosphorylation was found to largely attenuate the modulation of BmK AS on voltage-dependent kinetics for both $Na_v1.2\alpha$ and $Na_v1.2$ ($\alpha + \beta1$). It was of notice that the potency of PKA in reshaping the BmK AS pharmacological efficacy on sodium channel was in relevant to the different concentration of BmK AS, prominent for 1 nM and 100 nM, but less efficient for 10 nM. The inhibition rate on I_{Na} and negative shift of steady-state inactivation of $Na_v1.2\alpha$ induced by 10 nM BmK AS were even enhanced after PKA activation (Fig. 1D and Fig. 4B left, Pro AS). This exception was not occurred in the case when β1 subunit was co-expressed with $Na_v1.2\alpha$, in which there was a significant attenuation for 10 nM BmK AS-induced negative shifts in inactivation curves before PKA activation (Fig. 4 right, Pro AS). Finally, the remarkable increase in persistent Na^+ currents of sodium channel reported previously was hardly observed in our study before and after PKA phosphorylation, which was possibly due to the difference in BmK AS concentration used (500 nM in those researches)[14,24]. Based on the observations discussed above, the PKA phosphorylation and BmK AS modulation may be functionally related.

BmK AS belongs to β-like toxins that also includes AaH IT4 from *Androctonus australis* Hector (Loret et al., 1991) and Lqh β1 from *Leiurus quinquestriatus hebraeus* (Gordon et al., 2003). These toxins compete for the excitatory (AaHIT1, BmK IT) and depressant toxin (LqhIT2, BmK IT2) binding sites on sodium channels in insect neuronal preparations, as well as for site-4 of classical β-toxins on rat brain synaptosomes. Therefore, they are classified as "β-like toxins", but they also compete with moderate affinity with both α- and β-classical anti-mammalian toxins for their binding site (site 3 and 4) to rat brain synaptosomes[25–29]. The archetype of the β-like toxins is Ts1, from the Brazilian scorpion *Tityus serrulatus*. It was recently demonstrated that this toxin could cooperatively interact with three of four voltage-sensors in $Na_v1.2$ (domain II, III and IV) with different affinities, leading to opposite pharmacological consequences[30,31]. The same mechanism might exist and account for the unique pharmacological performance of BmK AS. Furthermore, the pattern of how BmK AS modulates sodium channel and the receptor sites on sodium channels might be conserved among β-like toxins.

Most of the PKA phosphorylation sites were located at DI-II loop and the C-terminal of VGSCs[2,32] which are right approximate to the ion permeable pore (DI S5–S6 and DIV S5–S6)[33,34].The action of PKA phosphorylation depends largely on the five consensus sites located in DI-II loop of VGSCs[4]. In addition, it is reported that the effects of PKA and PKC usually interact molecularly and physiologically, which was possibly owing to the shared phosphorylation

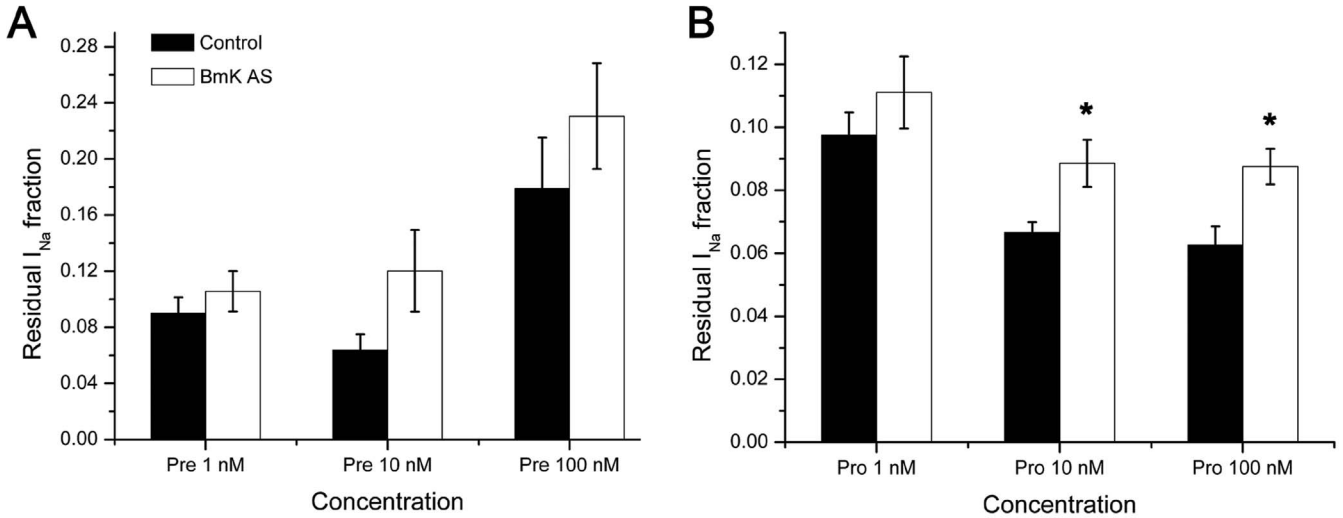

Figure 6 | The fractions of residual sodium current after depolarization to −20 mV for 10 ms in *Xenopus* oocytes, before (A) and after PKA phosphorylation (B)*$P < 0.05$; indicating significant difference between the control (white bar) and BmK AS (Dark bar) values.

site in DIII (N1466A)[35,36]. With refer to the pharmacological relevant of PKA phosphorylation and BmK AS modulation on $Na_v1.2$, although still arbitrarily based on current study, it may allow us to speculate that the attenuation of BmK AS potency on Na^+ currents by PKA phosphorylation might be due to an allosteric effect. However, more evidences from site-directed mutagenesis must be conducted to characterize this notion in depth.

Neuronal excitability is controlled much by the density of Na^+ currents, voltage-dependent activation and inactivation rate as a whole. Phosphorylation has long been considered as one of the upstream factors involving in regulating sodium channels and excitability of neurons. Evidences have showed that the synthesis of $Na_v1.7$ mRNA was disrupted when down-regulating the level of ERK-1/2 phosphorylation in adrenal medullary chromaffin cells[37]. Phosphorylation determines the efficiency of membrane insertion of $Na_v1.5$ channels, which could be irreversibly removed by protein trafficking inhibitor chloroquine and monensin[23]. Bao and her colleagues found that nociceptive factor prostaglandin E_2 was capable of promoting the $Na_v1.8$ trafficking via its intracellular RRR motif through the PKA pathway[38]. In prefrontal cortex spinal neurons, the endogenous Na^+ currents were inhibited by accelerated slow inactivation and decreased open probability of VGSCs after administration of PKA agonist cBMIP[35]. Our study demonstrated that the PKA phosphorylation may take part in the interactions between BmK AS and $Na_v1.2$, which could result in an attenuation effect on the potency of BmK AS modulation. In addition, by comparison of the responses of $Na_v1.2\alpha$ and $Na_v1.2$ (α + $\beta1$) to BmK AS, the differences in pharmacological consequences due to the different expression systems were hopefully to be explained in part. The availability of PKA phosphorylation and auxiliary subunits for sodium channels will provide new dimensions to evaluate the role of neurotoxins in modulating cell excitability.

Methods

Toxins and reagents. BmK venom was purchased from a individual scorpion farm in Henan Province, China. Toxins were purified by column chromatography from the crude venom of BmK as described previously[39]. The purity of the toxin was confirmed by mass spectrometry. Toxin powder was dissolved in water with 0.01 g/mL BSA and stored at −20°C.

Isoproterenol, the activator of PKA was purchased from Sigma, USA. Stock solutions of isoproterenol were made at a concentration of 100 mM in ND96 (in mM: NaCl 96, KCl 2, $CaCl_2$ 1.8, $MgCl_2$ 2 and HEPES 5, pH 7.5) and stored at −20°C.

Plasmids. The genes encoding the sodium channel α-subunit of rat VGSC isoform i.e. $Na_v1.2$ (CAA27287) and β_2 adrenalin receptor (β_2-AR) were originally from Dr. Alan L. Goldin (University of California, USA).

Transcription of NA and expression in *Xenopus* oocytes. The genes encoding the sodium channel α-subunit of rat VGSC isoform i.e. $Na_v1.2$ (CAA27287) and β_2 adrenalin receptor (β_2-AR) were originally from Dr. Alan L. Goldin (University of California, USA). All the plasmids were harvested in E.*coli* DH5 and sequenced. The gene for $Na_v1.2$ was transcribed *in vitro* using T7 NA-polymerase and the mMESSAGE mMACHINE™ system (Ambion, Austin, TX). β_2-AR NA was generated in vitro with SP6 NA–polymerase as the same procedure as that of $Na_v1.2$.

Xenopus laevis oocytes were prepared and injected with 10–20 ng of β2-AR and $Na_v1.2\alpha$cNA (1 : 2 weight ratios). Oocytes were incubated at 20°C for 2–5 days in ND96 solution (in mM: NaCl 96, KCl 2, $CaCl_2$ 1.8, $MgCl_2$ 2 and HEPES 5, pH 7.5), supplemented with 5 mM pyruvate and 0.1 mg/ml gentamicin.

$Na_v1.2$ and β_2-adrenergic receptor were co-expressed in *Xenopus* oocytes, which were clamped at −100 mV before electrophyiological recordings. Na^+ currents were induced in oocytes when depolarized to a series of step stimulus ranging from −100 mV to +70 mV. To minimize the individual difference between samples, only oocytes whose peak currents of I_{Na} were elicited at −20 mV or −30 mV were chosen for PKA phosphorylation.

Activation of PKA phosphorylation in oocytes. The bath solution consisted of ND-96 for all electrophysiological recordings. PKA was activated by perfusing oocytes that had been co-injected with β_2-AR NA with 100 μM Iso in bath solution for 10 min, which increased cytoplasmic cAMP levels and therefore activates PKA. The rate of perfusion with bath solution was carefully adjusted to 0.1 drop per second to minimize fluctuations in current amplitude resulting from changes in flow rate.

Electrophysiological recording and data analysis. Two-electrode voltage-clamp recordings were performed using Axon 900A amplifier (MDC, USA) and pclamp 10.0 software (MDC, USA). Data were acquired by Clampfit 10.3 (MDC, USA) and analyzed with Origin 7.5 (Northampton, USA) software. Voltage and currents electrodes were filled with 3 M KCl. Currents were filtered at 1.3 kHz and sampled at 10 kHz with a four-pole Bessel filter. Bath solution composition was (in mM): NaCl 96, KCl 2, $CaCl_2$ 1.8, $MgCl_2$ 2 and HEPES 5 (pH 7.4).

In *Xenopus* oocytes, the holding potentials were −100 mV. The I_{Na} were elicited by step pulses ranging from −100 to +70 mV for 100 ms with increments of 10 mV. The amplitudes of transient I_{Na} before and after BmK AS application were normalized to the peak I_{Na} before BmK AS application to generate the I–V curves. Mean conductance (G) was calculated from peak current/voltage relations using the equation $G = I/(V - Vr)$, where I is the peak current elicited upon depolarization, V is the membrane potential, and Vr is the reversal potential. The voltage dependence for the activation was fit with the Boltzmann relation, $G/Gmax = 1/[1 + \exp(V - V_m)/k_m]$, where V_m is the voltage for half-maximum activation and k_m is the slope factor. Current decays were fit with a double exponential equation: $I = A_{fast}*\exp[-(t - K)/\tau_{fast}] + A_{slow}*\exp[-(t - K)/\tau_{slow}] + I_{SS}$, where I is the current, A_{fast} and A_{slow} represent the percentage of channels inactivating with time constants τ_{fast} and τ_{slow}, K is the time shift, and I_{SS} is the steady-state asymptote.

The voltage dependence of fast inactivation and slow inactivation were analyzed by two-pulse protocols, composed of a 10 or 200 ms prepulse, respectively, to potentials ranging from −100 to +60 mV with the increments of 10 mV followed by a test pulse of −10 mV for 50 ms. Data were described with the two-state Boltzmann equation, $I/I_{max} = 1/[1 + \exp(V - V_{1/2})/k]$, where V is the membrane potential of the conditioning step, $V_{1/2}$ is the membrane potential at which half-maximal inactivation is achieved, and k is the slope factor. The parameters for fast inactivation were characterized by the half-maximal voltage V_f and the slope factor k_f; correspondingly V_s and k_s for slow inactivation.

The time constants of the development of slow inactivation were determined by fitting the data with a double exponential equation, $I/I_{max} = A_f * \exp(-t/\tau_f) + A_s * \exp(-t/\tau_s) + C$, where t is the conditioning pulse duration, A_{fast} and A_{slow} represent the percentage of channels inactivating with time constants τ_{fast} and τ_{slow} and C is the steady-state asymptote. The normalized currents I/I_{max} provided information about how many channels entered slow inactivation during the conditioning pulse.

Only recordings with leakage below 0.08 μA and fluctuation within 0.05 μA were selected in statistical analysis. Data are reported as mean ± SEM. Statistical significance between parameters of currents measured in control and toxin-containing solutions was assessed with Student's two-tailed paired *t* tests.

The effects of BmK AS took about 5–10 min to appear and more than 30 min to achieve a stable effect[14]. In this study, unless indicated, the effects of each concentration of toxin were examined after perfusion for 20 min.

1. Mao, J., Mayer, D. J., Hayes, R. L. & Price, D. D. Spatial patterns of increased spinal cord membrane-bound protein kinase C and their relation to increases in 14C-2-deoxyglucose metabolic activity in rats with painful peripheral mononeuropathy. *J Neurophysiol* **70**, 470–481 (1993).
2. Scheuer, T. Regulation of sodium channel activity by phosphorylation. *Semin Cell Dev Biol* **22**, 160–165 (2011).
3. Vijayaragavan, K., Boutjdir, M. & Chahine, M. Modulation of Nav1.7 and Nav1.8 peripheral nerve sodium channels by protein kinase A and protein kinase C. *J Neurophysiol* **91**, 1556–1569 (2004).
4. Smith, R. D. & Goldin, A. L. Phosphorylation at a single site in the rat brain sodium channel is necessary and sufficient for current reduction by protein kinase A. *J Neurosci* **17**, 6086–6093 (1997).
5. Murphy, B. J., Rogers, J., Perdichizzi, A. P., Colvin, A. A. & Catterall, W. A. cAMP-dependent phosphorylation of two sites in the alpha subunit of the cardiac sodium channel. *J Biol Chem* **271**, 28837–28843 (1996).
6. Ji, Y. H. *et al.* Covalent structures of BmK AS and BmK AS-1, two novel bioactive polypeptides purified from Chinese scorpion Buthus martensi Karsch. *Toxicon* **37**, 519–536 (1999).
7. Loret, E. P. *et al.* An anti-insect toxin purified from the scorpion Androctonus australis Hector also acts on the alpha- and beta-sites of the mammalian sodium channel: sequence and circular dichroism study. *Biochemistry* **30**, 633–640 (1991).
8. Li, Y. J. & Ji, Y. H. Binding characteristics of BmK I, an alpha-like scorpion neurotoxic polypeptide, on cockroach nerve cord synaptosomes. *J Pept Res* **56**, 195–200 (2000).
9. Tan, Z. Y., Chen, J., Shun, H. Y., Feng, X. H. & Ji, Y. H. Modulation of BmK AS, a scorpion neurotoxic polypeptide, on voltage-gated Na+ channels in B104 neuronal cell line. *Neurosci Lett* **340**, 123–126 (2003).
10. Wu, Y., Ji, Y. H. & Shi, Y. L. Sodium current in NG108-15 cell inhibited by scorpion toxin BmKAS-1 and restored by its specific monoclonal antibodies. *J Nat Toxins* **10**, 193–198 (2001).
11. Liu, T., Pang, X. Y., Jiang, F., Bai, Z. T. & Ji, Y. H. Anti-nociceptive effects induced by intrathecal injection of BmK AS, a polypeptide from the venom of Chinese-scorpion Buthus martensi Karsch, in rat formalin test. *J Ethnopharmacol* **117**, 332–338 (2008).
12. Zhao, R. *et al.* Anticonvulsant activity of BmK AS, a sodium channel site 4-specific modulator. *Epilepsy Behav* **20**, 267–276 (2011).
13. Chen, B. & Ji, Y. Antihyperalgesia effect of BmK AS, a scorpion toxin, in rat by intraplantar injection. *Brain Res* **952**, 322–326 (2002).

14. Zhu, M. M., Tao, J., Tan, M., Yang, H. T. & Ji, Y. H. U-shaped dose-dependent effects of BmK AS, a unique scorpion polypeptide toxin, on voltage-gated sodium channels. *Br J Pharmacol* **158**, 1895–1903 (2009).
15. Smith, R. D. & Goldin, A. L. Potentiation of rat brain sodium channel currents by PKA in Xenopus oocytes involves the I–II linker. *Am J Physiol Cell Physiol* **278**, C638–645 (2000).
16. Liu, Z. R. *et al.* Pharmacological kinetics of BmK AS, a sodium channel site 4-specific modulator on Nav1.3. *Neurosci Bull* **28**, 209–221 (2012).
17. Johnson, J. & Capco, D. G. Progesterone acts through protein kinase C to remodel the cytoplasm as the amphibian oocyte becomes the fertilization-competent egg. *Mech Dev* **67**, 215–226 (1997).
18. Smith, R. D. & Goldin, A. L. Functional analysis of the rat I sodium channel in xenopus oocytes. *J Neurosci* **18**, 811–820 (1998).
19. Moorman, J. R., Kirsch, G. E., VanDongen, A. M., Joho, R. H. & Brown, A. M. Fast and slow gating of sodium channels encoded by a single mRNA. *Neuron* **4**, 243–252 (1990).
20. Zhou, J. Y., Potts, J. F., Trimmer, J. S., Agnew, W. S. & Sigworth, F. J. Multiple gating modes and the effect of modulating factors on the microI sodium channel. *Neuron* **7**, 775–785 (1991).
21. Zhang, Z. *et al.* Kinetic model of Nav1.5 channel provides a subtle insight into slow inactivation associated excitability in cardiac cells. *PLoS One* **8**, e64286 (2013).
22. Gilles, N., Leipold, E., Chen, H., Heinemann, S. H. & Gordon, D. Effect of depolarization on binding kinetics of scorpion alpha-toxin highlights conformational changes of rat brain sodium channels. *Biochemistry* **40**, 14576–14584 (2001).
23. Zhou, J., Yi, J., Hu, N., George Jr, A. L. & Murray, K. T. Activation of protein kinase A modulates trafficking of the human cardiac sodium channel in Xenopus oocytes. *Circ Res* **87**, 33–38 (2000).
24. Tan, M., Zhu, M. M., Liu, Y., Cheng, H. W. & Ji, Y. H. Effects of BmK AS on Nav1.2 expressed in Xenopus laevis oocytes. *Cell Biol Toxicol* **24**, 143–149 (2008).
25. Cohen, L. *et al.* Direct evidence that receptor site-4 of sodium channel gating modifiers is not dipped in the phospholipid bilayer of neuronal membranes. *J Biol Chem* **281**, 20673–20679 (2006).
26. Gordon, D. *et al.* An 'Old World' scorpion beta-toxin that recognizes both insect and mammalian sodium channels. *Eur J Biochem* **270**, 2663–2670 (2003).
27. Chai, Z. F., Bai, Z. T., Liu, T., Pang, X. Y. & Ji, Y. H. The binding of BmK IT2 on mammal and insect sodium channels by surface plasmon resonance assay. *Pharmacol Res* **54**, 85–90 (2006).
28. Jia, L. Y., Zhang, J. W. & Ji, Y. H. Biosensor binding assay of BmK AS-1, a novel Na+ channel-blocking scorpion ligand on rat brain synaptosomes. *Neuroreport* **10**, 3359–3362 (1999).
29. Li, Y. J., Liu, Y. & Ji, Y. H. BmK AS: new scorpion neurotoxin binds to distinct receptor sites of mammal and insect voltage-gated sodium channels. *J Neurosci Res* **61**, 541–548 (2000).
30. Bosmans, F., Martin-Eauclaire, M. F. & Swartz, K. J. Deconstructing voltage sensor function and pharmacology in sodium channels. *Nature* **456**, 202–208 (2008).
31. Campos, F. V., Chanda, B., Beirao, P. S. & Bezanilla, F. beta-Scorpion toxin modifies gating transitions in all four voltage sensors of the sodium channel. *J Gen Physiol* **130**, 257–268 (2007).
32. Baek, J. H., Cerda, O. & Trimmer, J. S. Mass spectrometry-based phosphoproteomics reveals multisite phosphorylation on mammalian brain voltage-gated sodium and potassium channels. *Semin Cell Dev Biol* **22**, 153–159 (2011).
33. Catterall, W. A. Structure and function of voltage-gated ion channels. *Annu Rev Biochem* **64**, 493–531 (1995).
34. Catterall, W. A. From ionic currents to molecular mechanisms: the structure and function of voltage-gated sodium channels. *Neuron* **26**, 13–25 (2000).
35. Carr, D. B. *et al.* Transmitter modulation of slow, activity-dependent alterations in sodium channel availability endows neurons with a novel form of cellular plasticity. *Neuron* **39**, 793–806 (2003).
36. Chen, Y., Yu, F. H., Surmeier, D. J., Scheuer, T. & Catterall, W. A. Neuromodulation of Na+ channel slow inactivation via cAMP-dependent protein kinase and protein kinase C. *Neuron* **49**, 409–420 (2006).
37. Yanagita, T. *et al.* Destabilization of Na(v)1.7 sodium channel alpha-subunit mRNA by constitutive phosphorylation of extracellular signal-regulated kinase: negative regulation of steady-state level of cell surface functional sodium channels in adrenal chromaffin cells. *Mol Pharmacol* **63**, 1125–1136 (2003).
38. Luo, J., Marechal, J. D., Warmlander, S., Graslund, A. & Peralvarez-Marin, A. In silico analysis of the apolipoprotein E and the amyloid beta peptide interaction: misfolding induced by frustration of the salt bridge network. *PLoS Comput Biol* **6**, e1000663 (2010).
39. Ji, Y. H. *et al.* Two neurotoxins (BmK I and BmK II) from the venom of the scorpion Buthus martensi Karsch: purification, amino acid sequences and assessment of specific activity. *Toxicon* **34**, 987–1001 (1996).

Acknowledgements

This study was supported by the National Basic Research Program of China (2010CB529806), partially by grants from National Natural Science Foundation of China (31171064), Key Research Program of Science and Technology Commissions of Shanghai Municipality (11JC1404300) and National Postdoctoral Fellowship granted to L.Z. (2013M531186).

Author contributions

Conceived and designed the experiments: L.Z. and J.Y. Performed the experiments: L.Z., Z.H., W.J. Analyzed the data: L.Z. and Z.H. Contributed reagents/materials/analysis tools: Z.H. and Z.J. Wrote the paper: L.Z. and J.Y. All authors have reviewed the manuscript.

Additional information

Supplementary information accompanies this paper at http://www.nature.com/scientificreports

Competing financial interests: The authors declare no competing financial interests.

How to cite this article: Lui, Z.R., Zhang, H., Wu, J.Q., Zhou, J.J. & Ji, Y.H. PKA phosphorylation reshapes the pharmacological kinetics of BmK AS, a unique site-4 sodium channel-specific modulator. *Sci. Rep.* **4**, 3721; DOI:10.1038/srep03721 (2014).